AWES2020
20th Australasian Wind Engineering Society Workshop
8 – 9 April, 2021

Assessment of Upwind Terrain Categories of YMML using Gustiness Technique

Matthew B. Vallis, Nicholas K. Truong, Antonios W. Rofail
Windtech Consultants 607 Forest Road, Bexley, NSW 2007. reception@windtechglobal.com

ABSTRACT

The gustiness technique allows for an objective assessment of terrain categories based on the relationship between the mean wind speeds and gusts observed by the anemometer. With a view to improving design wind speed estimations, this study applies the gustiness technique to data observed at the Melbourne International Airport (YMML) for the most complete, published ABL model. Time-series of theoretical Terrain Category, TC, and gust correction factors, CF, were derived from the observed gust factors, *G*, of 1-hr and 10-min mean wind speeds. Averaging of these time-series from the 1-hr to 3-s model, show TCs for YMML vary from 1.2 to 3, and CFs from 0.94 to 1.16. TCs and CFs generated from the 10-min to 3-s model differ from 1-hr to 3-s results, requiring further investigation into the theoretical models of 10-min mean winds.

1. Introduction

Despite the open and flat terrain nature of aerodromes, a roughness length of z_0 = 0.02 m (TC 2 of AS/NZS 1170.2:2011) cannot be assumed for all wind directions due to bodies of water, varying lengths of grass and eventual upwind suburbs, bush, and other obstacles. An estimation of the effective roughness length of the terrain surrounding the anemometer can be made through the study of satellite photos, however results can vary wildly due to the subjective nature of the assessment and assumptions made in the transition between different terrain categories. The use of anemometric data to determine upwind roughness length or terrain category or turbulence intensity via analysis of gust factors, the ratio of peak gusts to mean wind speeds per wind sector as defined in Eq. (1), is by no means a novel approach. Masters et al. (2010) applied the technique to historical automated weather data observed at 148 locations along the southern and eastern seaboards of the U.S. Two distinct models were required due to the use of the Belfort 2000 cup anemometer which reported peak gusts as 5-s non-overlapping block-averages and the Vaisala 425 ultrasonic which reported gusts in the form of 3-s moving averages. Holmes (2016, 2017) applied the technique to data observed at 5 weather stations in and around Melbourne, however the effect of the mechanical filter on the frequency response of the cup anemometer was not considered. Safaei Pirooz et al. (2018) applied the technique to data observed at Wellington Airport for MK II cup and Vaisala WAA151 ultrasonic anemometers.

The abovementioned studies used 10-minute mean wind speeds and adopted different approaches in the determination of upwind roughness lengths, including the averaging of different parameters. Masters et al. (2010) used the Harris and Deaves (1981) variance model (Eq. 5) in combination with the von Kármán power density spectra (Eq. 6) (Greenway, 1979) in the determination of theoretical peak factors, *g*, but is not clear how integral turbulence length, *L*, was determined and whether the model gust factors developed varied with only height and roughness length or mean wind speed also. Regardless, averaged gust factors per wind direction were used to determine effective roughness lengths. The approach relies on comparing derived observed gust factors (Eq. 1) to gust factors as

determined by theoretical peak factors which vary with roughness length (Eq. 2). Holmes (2016, 2017) used a similar approach to determine the theoretical peak factors, however the AS/NZS 1170.2 (2011) definition of integral length scale, L_u = 85, was adopted for all wind speeds and roughness lengths. The averaging of observed data was performed on the turbulence intensity, *I*, as defined in Eq. (3), and a closed-form equation was used to estimate roughness length. Safaei Pirooz et al. (2018) performed a similar procedure to Holmes (2016, 2017), however gust factors were averaged when determining the roughness length per wind direction.

$$G = \frac{\widehat{U}_\tau}{U_T} \quad (1) \qquad \widehat{U}_\tau = U_T(1 + gI_u) \quad (2) \qquad I_u = \frac{\sigma_u}{U_T} \quad (3)$$

The present study applies the gustiness technique to the anemometric records located in Melbourne International Airport. It differentiates itself from other previous studies by: **1)** Adoption of the ESDU 85020 (1985) atmospheric boundary layer (ABL) model, considered to be the most sophisticated and accurate model for synoptic winds. **2)** Determination of TC and CF to Terrain Category 2, as defined by AS/NZS 1170.2 (2011) of z_o = 0.02m, to individual samples, with averaging performed on to time-series of *G*, TC and CF. **3)** Application of theoretical gust factor models of both 1-hr mean to 3-s gusts, G_{3600}, and 10-min means to 3-s gusts, G_{600}. **4)** Application of procedure for low and high wind speed thresholds.

2. Methodology

2.1 Determination of Gustiness Models

G were determined for a range of roughness lengths, z_o (1e-5 to 9.9 m; unitary intervals of the second significant figure), and mean wind speeds at *z* = 10m, *U* (0.1 to 50 m/s; intervals of 0.1 m/s), by application of the following procedure. Masters *et al.* (2010) was followed to determine standard deviation and spectral density function of wind at height z = 10m, for each combination of pre-defined values of *U* and z_o. However, in this study, *U* varies with z_o as per Harris and Deaves (1981), as given in Eq. (4), and L_u, required for the unfiltered von Kármán spectra in Eq. (6), is determined by Equations A2.14, A2.15 and A2.18 to A2.21 of ESDU 85020 (1985). Values of f and η in Eq. (5) are solved for a latitude of 40°.

$$U = 2.5u_*\left[\ln\left(\frac{z}{z_o}\right) + 5.75\left(\frac{z}{z_G}\right) - 1.88\left(\frac{z}{z_G}\right)^2 - 1.33\left(\frac{z}{z_G}\right)^3 + 0.25\left(\frac{z}{z_G}\right)^4\right] \quad (4)$$

$$\sigma_u = u_*\frac{7.5\eta\left[0.538 + 0.09\ln\left(\frac{z}{z_o}\right)\right]^{\eta^{16}}}{1 + 0.156\ln\left(\frac{u_*}{fz_o}\right)} \quad (5)$$

$$S_u(n) = {\sigma_u}^2\frac{4\frac{L_u}{U}}{\left[1 + 70.8\left(\frac{nL_u}{U}\right)^2\right]^{5/6}} \quad (6)$$

The determination of expected peak and gust factors of filtered spectrum follows the process outlined in Holmes and Ginger (2012). The transfer functions of Eqs. (7) and (8) represent the τ = 3-s running averaging filter of gusts, and mechanical response filter of the Synchrotac 706 cup anemometer of distance constant *D* = 13 m. An extra term is present in Eq. (8) to correct for missing low-frequency energy content for 10-min mean wind speed process. The Davenport (1964) peak factor in Eq. (11) is determined via calculation of the cycling rate, *v*, of Eq. (10) and standard deviation of the filtered

process, $\sigma_{u,f}$, of Eq.(9), which is divided by the unfiltered standard deviation of the wind, σ_u, to allow for the application of the unfiltered turbulence intensity when determining the gust factor in Eq.(12). For this study, height is fixed at z = 10m, gust averaging interval fixed at τ = 3 s, meaning the gust factor is a function of mean wind speed, U, sampling time, T (3600 s or 600 s) and roughness length, z_o.

$$|H_{T=3600s}(n)|^2 = \left[\frac{\sin(\pi n\tau)}{\pi n\tau}\right]^2 \frac{1}{1+\left(\frac{2\pi n\tau D}{U}\right)^2} \quad (7)$$

$$|H_{T=600s}(n)|^2 = \left\{\left[\frac{\sin(\pi n\tau)}{\pi n\tau}\right]^2 - \left[\frac{\sin(\pi nT)}{\pi nT}\right]^2\right\} \frac{1}{1+\left(\frac{2\pi n\tau D}{U}\right)^2} \quad (8)$$

$$\sigma_{u,f} = \left\{\int_0^\infty S_u(n)|H(n)|^2 dn\right\}^{1/2} \quad (9) \qquad \upsilon = \left\{\frac{\int_0^\infty n^2 S_u(n)|H(n)|^2 dn}{\int_0^\infty S_u(n)|H(n)|^2 dn}\right\}^{1/2} \quad (10)$$

$$g = \left\{\sqrt{2\ln(\upsilon T)} + \frac{0.577}{\sqrt{2\ln(\upsilon T)}}\right\}\frac{\sigma_{u,f}}{\sigma_u} \quad (11) \qquad G = 1 + g(U,T,z_o)I_u(U,z_o) \quad (12)$$

Peak and gust factors for both T=3600s and T=600s Synchrotac models are shown in Figure 1 for U=5 m/s, 10 m/s and 20 m/s over the most critical range of TCs [0 to 3, as defined by TC = 4 + $\log_{10}(z_o/2)$]. The peak factors vary little between TCs and are more sensitive to U and T, with higher wind speeds and longer sampling periods producing higher peak factors than lower wind speeds and lower sampling periods. Gust factors are sensitive to U, T and z_o, for TC (<2), but are less dependent on U for TCs rougher than TC 2. For the same range of U and TCs, a comparison of the standard deviation of the filtered process, σ_{uf}, shows variation with U and TC, but very little deviation of σ_{uf} between T=3600s and T=600s for the same combination of TC and U. An examination of the cycling rate also reveals near equal magnitudes for T=3600s and T=600s for the same U and TC, meaning the divergence in the peak factor and gust factor for different sampling periods is largely due to the T term in Eq (11).

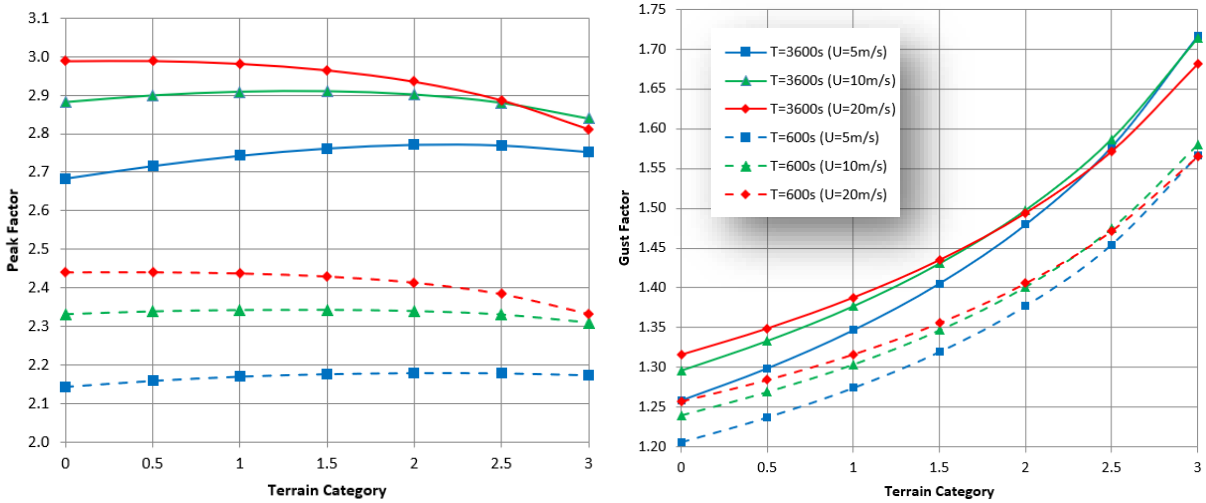

Figure 1. Peak and 3-s Gust Factors for Synchrotac 706 cup anemometer at z = 10m.

2.2 Description of Meteorological Data, Site and Determination of Directional Parameters

The analysis was based on 1-minute data (HD01D) obtained from the BoM for Melbourne International Airport (ICAO: YMML, WMO: 94866, BoM: 86282) from 19/10/1997 to 22/08/2016. During the almost 19-year period, the Synchrotac 706 anemometer was installed at a height of 10m above ground at LAT: -37.66347, LON: 144.83406 (BoM, 2018), the location of which is shown in Figure 2 with a 2km radius. At 1-minute intervals, the following data is reported: 1-minute mean wind speed, V, predominant wind

direction over 1 minute, *DIR*, highest maximum 3-s wind gust over 1 minute, V_{3s}. The *V* and *DIR* time-series were used to generate 10-minute means (U_{600s}, D_{600s}) and 1-hr means (U_{3600s}, D_{3600s}) at the same timestamps of 1-minute intervals. Corresponding 3-s gust factor time-series were also generated (G_{600s}, G_{3600s}) based on the highest V_{3s} over the previous 600-s and 3600-s periods. Values of U_T, D_T and G_T for which more than 30% of the reported data was missing or invalid were excluded from further analysis. To ensure the analysis was performed for conditions of neutral atmospheric stability associated with synoptic winds, standard deviations of the mean wind speeds, σ_{UT}, and wind direction, σ_{DT}, were calculated for each time interval and samples for which $(V_{3s}\text{-}U_T)/\sigma_{UT} > 5$ were or $\sigma_{DT} > 10°$ removed. Instances in which the scalar and vector U_T values differed by more than 0.51 m/s were also removed. Analysis of stationary wind events is necessary, and although the above filters eliminate many non-stationary convective storm events, some may remain in the sample but are expected to have a negligible impact on results.

For each of the 36 wind sectors (intervals of 10°, sweep of ±10°), G_T were calculated and analysed for two different mean wind speed thresholds: $U_T > 5$ m/s and top 1% U_T. Top 1% U_T threshold ranges from ≈15 m/s for northerly winds ($D_T = 0°$) to ≈8 m/s for the less frequent easterly winds ($D_T = 90°$). For each valid timestamp the theoretical model for the Synchrotac cup anemometer, as described in Section 2.1, was consulted to match the combination of U_T and G_T with z_o. Once matched with z_o, the corresponding TC was determined. The CF is ratio of the theoretically ideal peak 3-s gust wind speed (*T*, *z*=10m, z_o=0.02, *D*=0) to the observed peak 3-s gust over period *T* minutes (*T*, *z*=10m, z_o, *D*=13). CF determination per timestamp requires matching the gradient height wind speed, *U* at $z=z_G$ (Eq.4), of G_T with that of a theoretically ideal gust model, i.e., no anemometer cup filter, *D*=0m, in standard open terrain of z_o = 0.02m. The means and std of time-series of each derived parameter, *G*, TC and CF, were determined per wind sector for mean wind speeds of *T*=600s and *T*=3600s and two different mean wind speed thresholds.

3. Results

Polar plots of the mean and mean + standard deviation directional results are shown in Figure 2 for Gust Factors (GF), Figure 3 for Terrain Categories (TC) and Figure 4 for Gust Correction Factors to z_o = 0.02 m (CF). To best allow for visual comparison, results for different *U* thresholds (low: *U* > 5m/s, high: top 1% of *U*) are shown on separate plots, while results for the two different *T* periods are shown on the same polar plot. A qualitative analysis of the mean GFs of Figure 2 meet expectations: higher values of G_{3600s} over G_{600s}, high values for the north-western sectors where there is dense bush, lower values from the north and south-eastern sectors which align with the length of the long and smooth 16/34 runway. Directional plots are smoother for the low threshold *U* which vary by ±5% of *G* of higher threshold *U* (excluding wind directions 50-130° for which there were few samples).

Theoretically, TCs generated by analysis of G_{3600s} and G_{600s} should converge, however there is no agreeance between the derived TCs per wind direction as shown in Figure 3, for either the low or high *U* thresholds. Mean TCs from G_{600s} are 0.5 TC lower on average than those generated from G_{3600s}. Since the Harris and Deaves (1981) ABL model of Eq.(4) is based on wind speeds averaged over an hour, it follows that greater confidence is assigned to results derived from the analysis of G_{3600s}, leading to the assumption of gaps in the theoretical approach to generating gust factors for other averaging intervals, e.g., 10-minute means. Figure 3 shows the temporal variation of calculated gust factors for which the average standard deviation is 0.6 TC for high threshold *U*, and 0.7 for low threshold *U* (G_{3600s} model). A comparison between TCs of high and low *U* thresholds for the G_{3600s} model shows that TCs from the low *U* threshold analysis vary between -0.5 TC to +0.3TC to those from the analysis of high threshold *U*, with average of -0.2 TC (excluding wind directions 50-130°). TC results of Holmes (2016) are plotted in Figure 3 for comparison. They generally agree well with the TC results for high threshold *U* and G_{3600s}, except for the northerly winds, for which Holmes (2016) overestimates roughness by ≈ 1 TC.

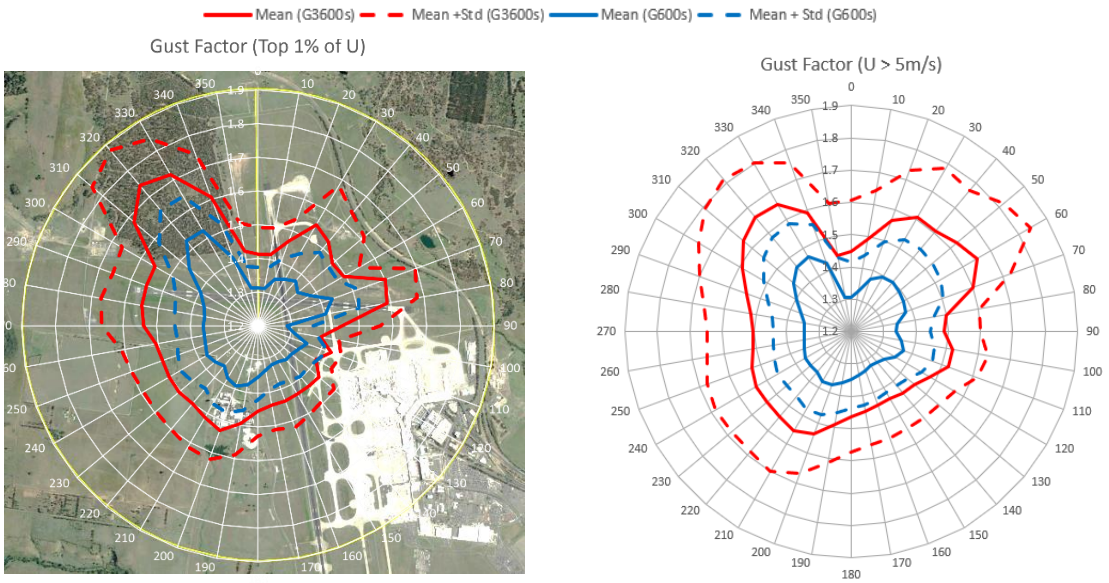

Figure 2. 3-s Gust Factors of YMML

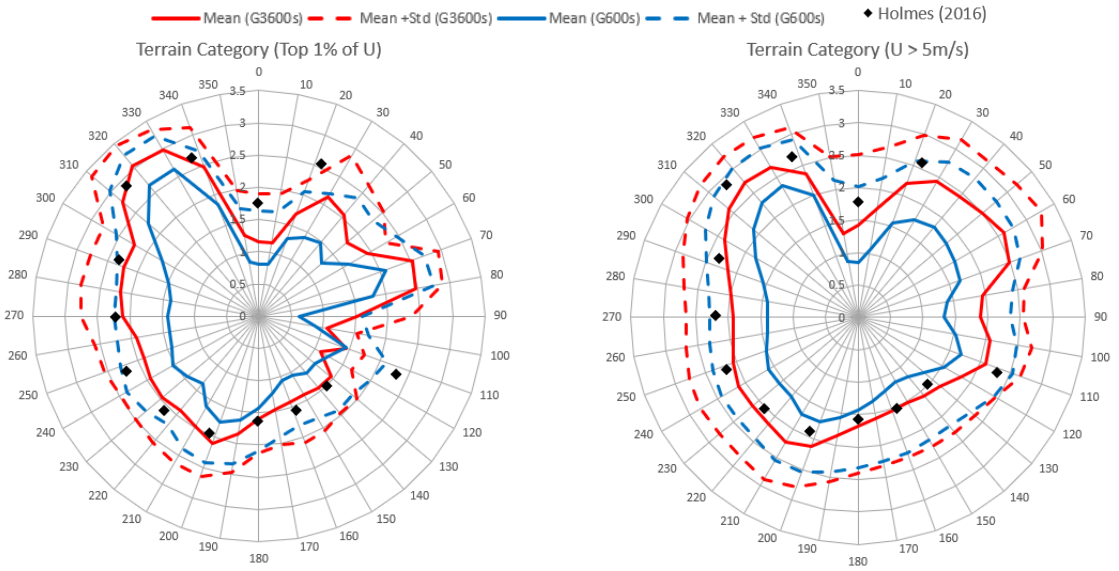

Figure 3. Assessed Terrain Categories of YMML

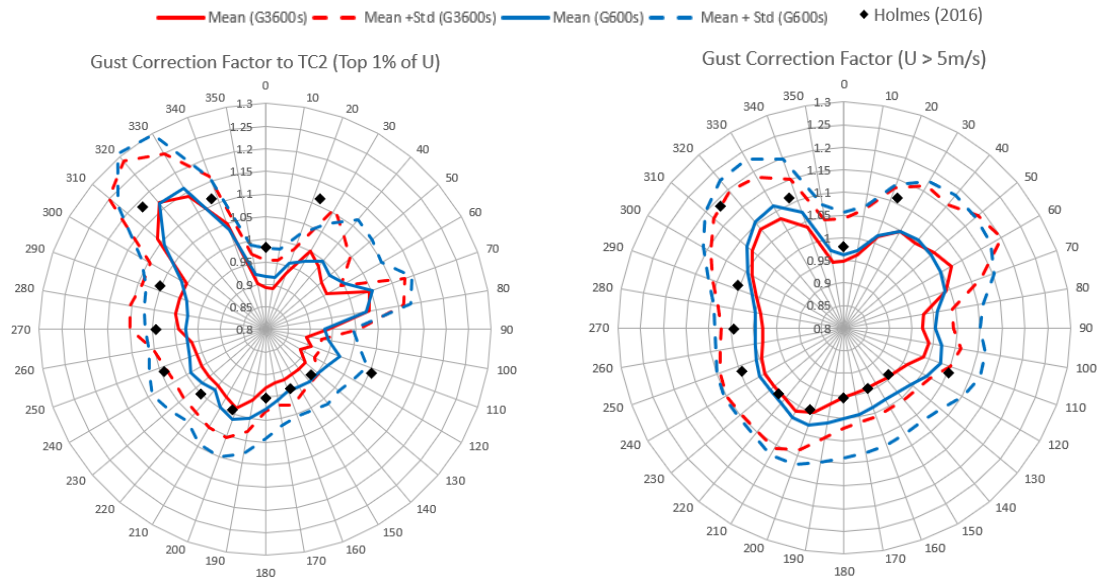

Figure 4. Assessed 3-s Gust Correction Factors to TC2 of YMML

The impact of the different TC assessments on potential design wind speeds is shown in the polar plots of gust correction factors of Figure 4. The CF from the analysis of G_{3600s} for high U threshold based for the 3 predominant wind directions of Melbourne are 0.89 (0°), 0.93 (180°) and 0.99 (270°). The corresponding CFs from analysis of G_{600s} are 0.92 (0°), 0.98 (180°) and 0.98 (270°). Good agreement is found between averaging periods for the northern and western wind directions; however, a 5% difference is evident for the westerly winds. An analysis of the difference between these CFs (CF_{600s}/CF_{3600s}) per TC (from G_{3600s} analysis), as plotted in Figure 5, shows a weak correlation between TC and difference in CF.

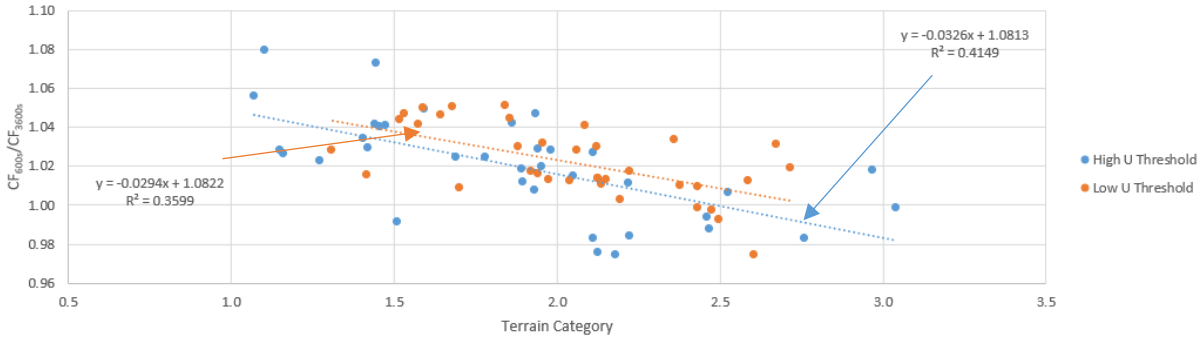

Figure 5. Ratio of derived gust CF_{600s} to CF_{3600s} plotted against TC from assessment of G_{3600s}.

The standard deviation of the scatter in Figure 5 is 2%, meaning there is generally good agreement between CF_{3600s} and CF_{600s}. However, a weak, linear relationship exists between the ratio of correction factors. For TCs > 2.5, $CF_{3600s} > CF_{600s}$, whilst the opposite is true for TCs<2.5. This trend holds for both the high and low threshold U analyses, and should be studied in greater detail to bridge any possible "gap" between the theoretical wind models of sampling periods less than 1 hour.

4. Conclusions

Theoretical gust factor models were determined for Australia's observing protocols, defined as a functions of mean wind speed, roughness length and mean wind speed averaging interval. The gustiness technique was applied to meteorological data observed at YMML and analysed mean gust factors, terrain categories and gust correction factors were determined for 36 wind directions. Differences between mean wind speed threshold and averaging interval were noted, with further investigation required to identify the apparent gap in the determination of theoretical peak factors for mean wind speeds averaged over a period less than 1 hour.

References

Bureau of Meteorology, (2018), Private communication, received 11/10/2018.

Davenport, A.G., (1964), Note on the distribution of the largest value of a random function with application to gust loading. Proceedings of the Institution of Civil Engineers, vol.28:187-196.

Engineering Science Data Unit 85020, (1985), Characteristics of atmospheric turbulence near the ground, Part II: single point data for strong winds (neutral atmosphere), with Amendments A to G, August 2001.

Greenway, M.E., (1979), An analytical approach to wind velocity gust factors, Journal of Wind Engineering and Aerodynamics vol.5:61-91.

Harris, R.I., Deaves, D.M., (1981), The structure of strong wind. *Proceedings of the CIRIA Conference on Wind Engineering in the Eighties*, 12-13 November 1980, CIRIA, London.

Holmes, J.D., Ginger J.D., (2012), The gust wind speed duration in AS/NZS 1170.2. Australian Journal of Structural Engineering, vol.13/3:207-218.

Holmes, J.D. (2016), Determination of turbulence intensity and roughness length from AWS data. *Proceedings of the 18th Australasian Wind Engineering Society Workshop*, McLaren Vale, Australia, Jul 6-8, 2016.

Holmes, J.D. (2017), Roughness lengths and turbulence intensities for wind over water. *Proceedings of the 9th Asia-Pacific Conference on Wind Engineering*, Auckland, New Zealand, Dec 3-7, 2017.

Masters, F.J., Vickery, P.J., Bacon, P., Rappaport, E.N (2010), Toward Objective, Standardized Intensity Estimates from Surface Wind Speed Observations. *Bulletin of the American Meteorological Society* vol. 91/12:1665-1681.

Safaei Pirooz, A.A., Flay, R.G.J., Turner, R. (2018), Effects of site relocation and instrument type on recorded wind data characteristics at Wellington Airport. *Proceedings of the 18th Australasian Wind Engineering Society Workshop*, McLaren Vale, Australia, Jul 6-8, 2016.

Standards Australia, (2011), "Structural design actions. Part 2 Wind actions", Australian/New Zealand Standard, AS/NZS 1170.2:2011 with Amendments 1 to 4.